Timescale for MeV electron microburst loss during geomagnetic storms

R. M. Thorne,[1] T. P. O'Brien,[2] Y. Y. Shprits,[1] D. Summers,[3] and R. B. Horne[4]

Received 3 November 2004; revised 6 April 2005; accepted 10 April 2005; published 1 September 2005.

[1] Energetic electrons in the outer radiation belt can resonate with intense bursts of whistler-mode chorus emission leading to microburst precipitation into the atmosphere. The timescale for removal of outer zone MeV electrons during the main phase of the October 1998 magnetic storm has been computed by comparing the rate of microburst loss observed on SAMPEX with trapped flux levels observed on Polar. Effective lifetimes are comparable to a day and are relatively independent of L shell. The lifetimes have also been evaluated by theoretical calculations based on quasi-linear scattering by field-aligned waves. Agreement with the observations requires average wide-band wave amplitudes comparable to 100 pT, which is consistent with the intensity of chorus emissions observed under active conditions. MeV electron scattering is most efficient during first-order cyclotron resonance with chorus emissions at geomagnetic latitudes above 30 degrees. Consequently, the zone of MeV microbursts tends to maximize in the prenoon (0400–1200 MLT) sector, since nightside chorus is more strongly confined to the equator.

Citation: Thorne, R. M., T. P. O'Brien, Y. Y. Shprits, D. Summers, and R. B. Horne (2005), Timescale for MeV electron microburst loss during geomagnetic storms, *J. Geophys. Res.*, *110*, A09202, doi:10.1029/2004JA010882.

1. Introduction

[2] Chorus emissions are intense whistler-mode waves, which are excited in discrete bursts following the injection of plasmasheet electrons into the region outside the plasmapause during enhanced convection. The properties of chorus have been described in previous studies [e.g., *Tsurutani and Smith*, 1977; *Meredith et al.*, 2003; *Santolik et al.*, 2003]. Chorus emissions are important because of their strong interaction with electrons in the outer radiation belt, which leads to nonadiabatic scattering. For pitch angles in the vicinity of the loss cone, such scattering leads to precipitation into the atmosphere and a net removal of energetic electrons from the outer radiation zone. The inherently bursty nature of chorus [*Tsurutani and Smith*, 1977; *Santolik et al.*, 2003] causes microbursts of precipitation, which can be measured on low-altitude satellites such as SAMPEX [*Lorentzen et al.*, 2001; *O'Brien et al.*, 2003, 2004]. Comparison of the precipitation flux with the trapped content of the radiation belts has shown that chorus-induced microbursts could substantially deplete the MeV electron outer radiation belt during the 1–2 day duration of a magnetic storm. Microburst precipitation tends to be far more intense during the storm main phase, but it can persist during the storm recovery, in competition with acceleration processes that lead to a net flux enhancement [*O'Brien et al.*, 2004]. Quantification of electron microburst loss is therefore important before an accurate assessment can be made of relevant acceleration processes.

[3] The principal purpose of this study is to quantify the rate of microburst loss for relativistic electrons and to compare the estimated lifetimes with theoretical calculations based on quasi-linear scattering. Specifically, we wish to identify the preferred spatial location for scattering and the L shell dependence of computed lifetimes and to determine the required power spectral intensity of waves to account for this loss. Data from SAMPEX and Polar are combined to obtain an estimate of lifetimes during the main phase of the October 1998 storm (section 2). A simplified formulation of pitch angle diffusion is given in section 3, and numerical results are presented in section 4. We conclude with a discussion of the relative importance of microburst precipitation compared with other loss processes in different phases of a storm.

2. Calculation of MeV Electron Lifetimes From Microbursts

[4] The calculation of MeV electron lifetimes due to microbursts requires data from two orbiting satellites. First, the number of trapped electrons per unit L is calculated from fluxes observed at Polar. Then, the number of electrons being lost per unit time over a small range of L is calculated from microburst fluxes observed at low altitude on SAMPEX. The trapped content in that small L

[1]Department of Atmospheric and Oceanic Sciences, University of California, Los Angeles, California, USA.
[2]Space Science Department, The Aerospace Corporation, El Segundo, California, USA.
[3]Department of Mathematics and Statistics, Memorial University of Newfoundland, St. John's, Newfoundland, Canada.
[4]British Antarctic Survey, Natural Environment Research Council, Cambridge, UK.

0148-0227/05/2004JA010882

Table 1. Electron Pitch Angle Indices $\sin^{n_L}\alpha$ and Microburst Occurrence $C_{\rm mb}(L)$ at Each L Shell

L	n_L	$C_{\rm mb}(L)$
2.00		0.0007
2.25		0.0004
2.50		0.0004
2.75		0.0008
3.00	5.380	0.0016
3.25	5.078	0.0093
3.50	4.669	0.0349
3.75	3.916	0.0746
4.00	3.095	0.1463
4.25	2.495	0.2335
4.50	2.151	0.2875
4.75	1.998	0.3132
5.00	1.899	0.3150
5.25	1.942	0.2833
5.50	1.974	0.2326
5.75	1.939	0.1745
6.00	1.970	0.1184
6.25	2.136	0.0748
6.50	1.970	0.0545
6.75	1.438	0.0337
7.00	1.254	0.0182
7.25	1.194	0.0145
7.50	1.046	0.0082
7.75	0.989	0.0028
8.00	0.852	0.0038
8.25		0.0005
8.50		0.0019
8.75		0.0029
9.00		0.0030

range is then compared with the loss rate to determine an effective lifetime for microburst loss.

2.1. Relativistic Trapped Electron Content

[5] Assuming gyrotropy, we model the equatorial perpendicular trapped flux as $j_\perp^{(\rm eq)}(E, L) = a_L E^{-d_L}$. Polar data is used to obtain a_L and d_L, assuming a dipole field and a $sin^{n_L}\alpha$ pitch angle distribution. The pitch angle index n_L at each L shell (given in Table 1) is taken from earlier measurements by *Vampola* [1996]. The relativistic electron content at each L shell can then be obtained from the integral

$$\frac{\partial N_{rel}}{\partial L} = 2\pi mc \int_{1\rm MeV}^{\infty}\int_0^{\pi} \frac{E+1}{(E(E+2))^{1/2}} \sin^{n_L+1}\alpha j_\perp^{(\rm eq)}(E,L) \cdot \frac{\partial V}{\partial L} dE d\alpha, \quad (1)$$

where the electron energy E is measured in rest mass units (mc^2) and the L shell volume for a dipole field is (corrected from *Lyons and Williams* [1984])

$$V = \frac{4\pi R_E^3}{105}\sqrt{1-1/L}\left(16L^3 + 8L^2 + 6L - 30\right). \quad (2)$$

The dipole approximation (2) is accurate at low L but will tend to underestimate V near geostationary orbit, possibly by as much as 40%.

2.2. Estimation of MeV Electron Microburst Loss

[6] The HILT/SSD instrument on SAMPEX measures electrons above 1 MeV with a 20-ms resolution. The local precipitation flux attributed to microbursts can be obtained by subtracting the spiky portion of the flux time series from a smooth baseline which corresponds to particles in the drift-loss cone and hence not locally precipitating [e.g., *O'Brien et al.*, 2004]. Using this integral unidirectional microburst flux $J_{\rm mb}(L)$, the loss rate of >1 MeV electrons is

$$\frac{dN_{rel}}{dt} = J_{\rm mb}(L)A(L)\Omega. \quad (3)$$

We assume that precipitation appears over $\Omega = 2\pi$ steradians in either hemisphere. $J_{\rm mb}(L)$ is a 20-ms average over the small latitude range (λ_1 to λ_2) traversed by SAMPEX during each sample. To estimate the corresponding area $A(L)$ for precipitation loss, we further assume that the microbursts are confined to 6 hours of MLT based on the statistical size of the microburst precipitation region [*O'Brien et al.*, 2004]. Consequently, $A(L) = 2|\sin\lambda_2 - \sin\lambda_1|(\pi/2)\,R^2$, where R is the nearly constant distance from SAMPEX to the center of the Earth, and the factor of two comes from assuming the conjugate hemisphere sees similar microburst precipitation. The rate of relativistic electron precipitation loss is

$$\frac{dN_{rel}}{dt} = 2\pi^2 R^2 J_{\rm mb}(L)|\sin\lambda_2 - \sin\lambda_1|. \quad (4)$$

The corresponding change in L shell range ΔL over the 20-ms sample can be obtained from the SAMPEX telemetry.

2.3. Calculation of Effective Lifetime

[7] The Polar and SAMPEX observations yield an instantaneous microburst lifetime

$$T = \frac{\partial N_{rel}/\partial L}{dN_{rel}/dt}\Delta L. \quad (5)$$

However, this must be adjusted to account for the occurrence $C_{mb}(L)$ of microbursts as a function of L in the 6-hour dawn sector (where the microbursts are observed) and also for overcounting Q of backscattered microbursts on the second and subsequent bounces. Note that the HILT instrument has a poor angular resolution (due to its large geometric factor) and cannot resolve the local bounce loss cone [*Blake et al.*, 1996]. The effective lifetime from microburst precipitation into the bounce loss cone is therefore

$$\tau_{\rm mb} = T \times Q/C_{mb}(L). \quad (6)$$

The microburst occurrence $C_{mb}(L)$ is based on SAMPEX observations in the dawn sector taken from the $Kp = 4$–6 statistics given in Table 1. Lower values of $C_{mb}(L)$ indicate less frequent microbursts and thus longer effective lifetimes. The overcounting Q is obtained by the assumption that a fraction q of the microburst flux survives each bounce into the upper atmosphere. We estimate that q is 0.675 based on the observation that an isolated bouncing microburst [*Blake et al.*, 1996] exhibited a drop to 0.14 of its original value on its third return to SAMPEX. This third return could include two or three visits to the opposite hemisphere. We thus assume that the microburst had visited the atmosphere five

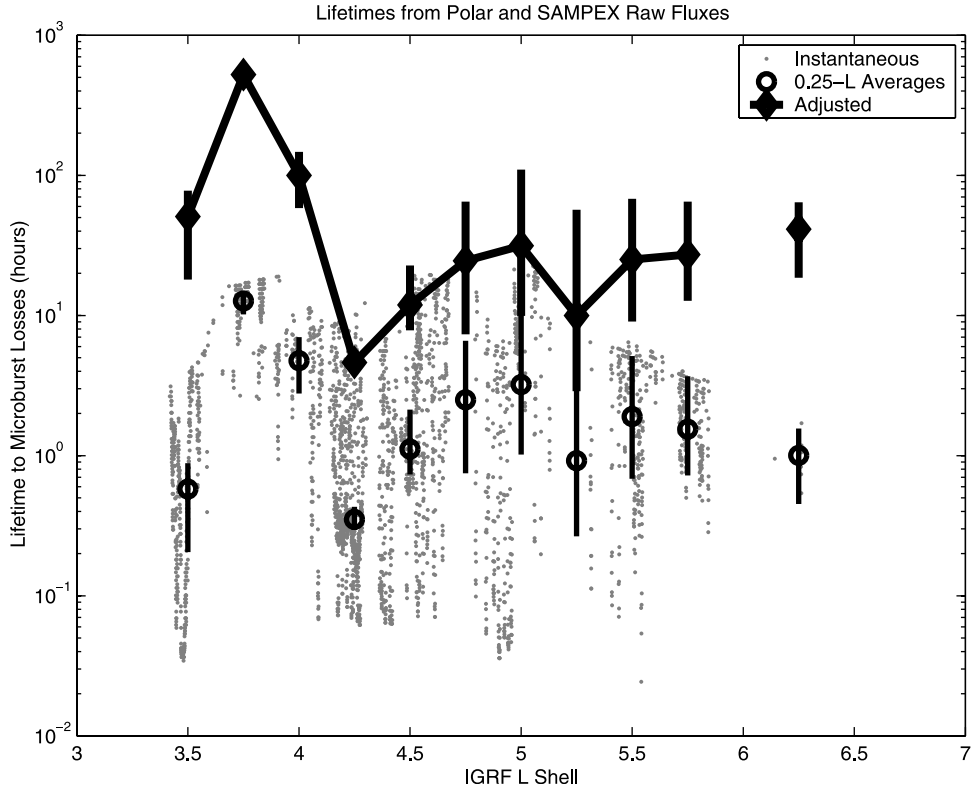

Figure 1. Microburst lifetimes obtained from a comparison of precipitation flux observed on SAMPEX with trapped flux on Polar during the main phase of the October 1998 storm. Instantantaneous values were deduced from 20 ms resolution data of microbursts observed by the HILT instrument on SAMPEX. This was adjusted for microburst occurrence rate and oversampling to obtain average lifetimes as a function of L.

times, giving $q = 0.14^{1/5} = 0.675$. Assuming that each given flux spike, identified as a microburst, is actually an infinite superposition of attenuated returns of previous bursts, the oversampling correction factor Q is then given by

$$Q = \sum_{n=0}^{\infty} q^n = 1/(1-q) = 3.1. \tag{7}$$

[8] Results from this analysis of microburst lifetimes are shown in Figure 1 as a function of L shell. There is considerable scatter in the instantaneous lifetimes T obtained from the 20-ms data samples on SAMPEX. Use of the dipole approximation to obtain V could cause an underestimate of lifetimes by as much as 30% at geostationary orbit, but such errors are much less at lower L. Averages over a 0.25 L shell range are better ordered and more representative of average loss times when microbursts are active. The adjusted lifetimes (6) shown by the heavy solid line, which takes into account the occurrence rate of microbursts and overcounting, indicate little systematic change with L, especially over the region where microburst occurrence is high ($L > 4$). The center points are median lifetimes and the error bars are 95% confidence intervals generated using Monte Carlo resampling with an exponential inflation factor of 3 added afterward to account for the strong serial correlation in the time series. The average lifetime during this storm was about a day. The much lower occurrence rate of microburst at low $L < 4$ is probably related to changes in the location of the plasmapause during the storm.

3. Pitch Angle Diffusion Rate

[9] Resonant wave-particle scattering can occur whenever the wave frequency ω is Doppler-shifted to some multiple of the relativistic electron gyrofrequency:

$$\omega - k_{\|} v_{\|} = n\Omega_e/\gamma. \tag{8}$$

Diffusion codes have recently been developed [*Horne et al.*, 2003a, 2005; *Albert*, 2005; *Glauert and Horne*, 2005] to evaluate the bounce-averaged rate of pitch angle scattering. Such codes evaluate the scattering at the Landau ($n = 0$) resonance and each cyclotron harmonic for a prescribed distribution of wave power. Other key inputs to the codes are models for the distribution of magnetic field and plasma density. For an arbitrary distribution of wave energy, scattering by many harmonic resonances needs to be carefully evaluated and, when bounce-averaging is performed, this tends to require a large amount of CPU time [*Horne et al.*, 2005]. However, the propagation vectors of chorus emissions observed on Cluster are predominantly field-aligned in the equatorial source region [*Santolik et al.*, 2003]. For nearly field-aligned waves, first-order cyclotron resonant scattering dominates over other resonances. We take advantage of this property to construct a simple

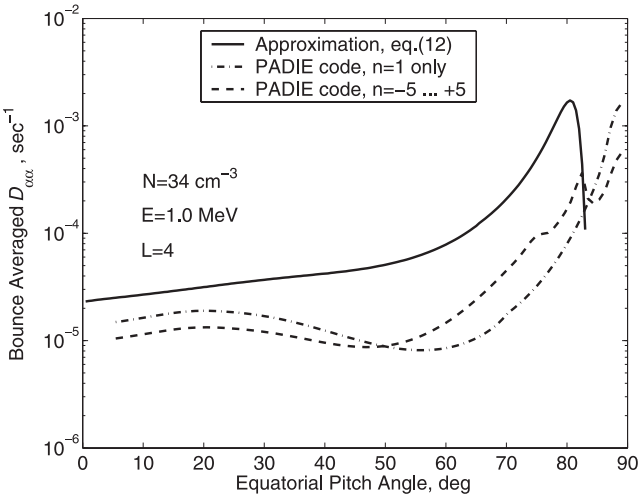

Figure 2. Comparison between exact solution for the bounce-averaged rate of pitch angle diffusion and our approximate values for first-order cyclotron resonance with field-aligned waves. Diffusion rates near the loss cone agree within a factor of two.

analytic expression for the local rate of pitch angle scattering to evaluate diffusion rates near the loss cone. By direct comparison with results from the exact PADIE (Pitch Angle and Energy Diffusion of Ions and Electrons) diffusion code [*Glauert and Horne*, 2005], we show that this simple analytic treatment gives results accurate to within a factor of two near the loss cone. This is acceptable for the determination of lifetimes, since there is larger uncertainty in the measured lifetimes and in the properties of the waves. One obvious advantage of using the analytic solution is the ability to rapidly test the sensitivity of computed lifetimes to the adopted model parameters, such as the plasma density distribution and the latitudinal distribution of the waves.

[10] To evaluate the rate of pitch angle scattering by chorus emissions, we assume that the wave energy is distributed over a Gaussian frequency distribution

$$B^2(\omega) = A_w^2 \exp -\left(\frac{\omega - \omega_m}{\delta\omega}\right)^2, \tag{9}$$

where $B^2(\omega)$ is the power spectral density of the wave magnetic field (in nT^2 Hz^{-1}), ω_m and $\delta\omega$ are the frequency of maximum wave power and bandwidth, respectively (in rads s^{-1}), and

$$A_w^2 = \frac{|B_w|^2}{\delta\omega}\,\frac{2}{\sqrt{\pi}}\left(\mathrm{erf}\left(\frac{\omega_m - \omega_{lc}}{\delta\omega}\right) + \mathrm{erf}\left(\frac{\omega_{uc} - \omega_m}{\delta\omega}\right)\right)^{-1}. \tag{10}$$

B_w is in units of nT. The wave spectrum is also bounded by upper ω_{uc} and lower ω_{lc} frequency limits and is set to zero outside these limits.

[11] We also assume that the chorus waves are field-aligned so that scattering is entirely due to the first harmonic cyclotron resonance [e.g., *Lyons et al.*, 1971]. With the additional approximation that the wave frequency can be ignored compared to the electron gyrofrequency in both the wave dispersion relationship so that

$$\omega = \frac{k^2 c^2 \Omega_e}{\omega_p^2} \tag{11}$$

and in the resonance condition (8), the local rate of pitch angle scattering $D_{\alpha\alpha}$ can be written as a simple analytic expression

$$D_{\alpha\alpha} = \frac{\pi\Omega_e\omega_{res}}{\nu\delta\omega(E+1)}\left(\frac{B_w}{B_0(\lambda)}\right)^2 \exp -\left(\frac{\omega_{res} - \omega_m}{\delta\omega}\right)^2, \tag{12}$$

where E is again measured in units of mc^2, $B_0(\lambda)$ is the local magnetic field strength, $\nu = 1.764$ assuming cut-off for the wave power at $\omega_{lc} = \omega_m - 2\delta\omega$ and $\omega_{uc} = \omega_m + 2\delta\omega$, and the resonant wave frequency

$$\omega_{res} = \frac{\alpha^\star\Omega_e}{E(E+2)cos^2\alpha}. \tag{13}$$

Here $\alpha^\star = (\Omega_e/\omega_{pe})^2$ is an important dimensionless parameter which controls the resonance condition.

[12] It is usually most convenient to classify trapped particles by their energy and equatorial pitch angle α_{eq}. As electrons move along their quasi-adiabatic bounce orbits, both their pitch angle and the local cyclotron resonant frequency (13) will change. The bounce-averaged rates of diffusion [e.g., *Lyons et al.*, 1972] are given by

$$\langle D_{\alpha_{eq}\alpha_{eq}}\rangle = \frac{1}{T(\alpha_{eq})}\int_0^{\lambda_m} D_{\alpha\alpha}\frac{\cos\alpha}{\cos^2\alpha_{eq}}\cos^7\lambda d\lambda, \tag{14}$$

where

$$T(\alpha_{eq}) = \frac{\nu\tau_b(\alpha_{eq})}{4LR_E} = 1.30 - 0.56\sin\alpha_{eq}, \tag{15}$$

λ_m is the mirror latitude of the electrons, v is the electron velocity, and $\tau_b(\alpha_{eq})$ is the bounce period in a dipole magnetic field.

4. Numerical Results

[13] We use our analytical expression (12) for $D_{\alpha\alpha}$ to evaluate the local rate of pitch angle scattering at different latitudes along the quasi-adiabatic bounce orbits of electrons with a prescribed energy and equatorial pitch angle. These results are then bounce-averaged using (14) to obtain the effective scattering rates near the edge of the loss cone. Owing to scattering by chorus waves, trapped electron flux will be subject to exponential decay over a lifetime comparable to the inverse of the diffusion rate near the edge of the loss cone [e.g., *Thorne et al.*, 2005]. Consequently, we estimate that $\tau_{mb} \sim 4/\langle D_{\alpha_{eq}\alpha_{eq}}(\alpha_{LC})\rangle$; the factor of 4 comes from drift averaging over the 6 hours of MLT where microburst scattering is most effective. We adopt realistic parameters for the stormtime properties of lower-band equatorial chorus (ω_m = 0.35 Ω_e, $\delta\omega$ = 0.15 Ω_e, B_w = 100 pT), based on the statistical study of *Meredith et al.* [2003]. The trough plasma density model of *Sheeley et al.* [2001], $N = 124\ (3/L)^4$ cm^{-3}, is used to simulate equatorial conditions outside the plasmapause. Density models involving two latitudinal variations are used, the first having constant density with latitude and the second with $N(\lambda) \sim B_0(\lambda)$. These represent extreme bounds, with the former being more realistic.

[14] We first consider the accuracy of using the simple analytic expression (12) by comparing (see Figure 2) our

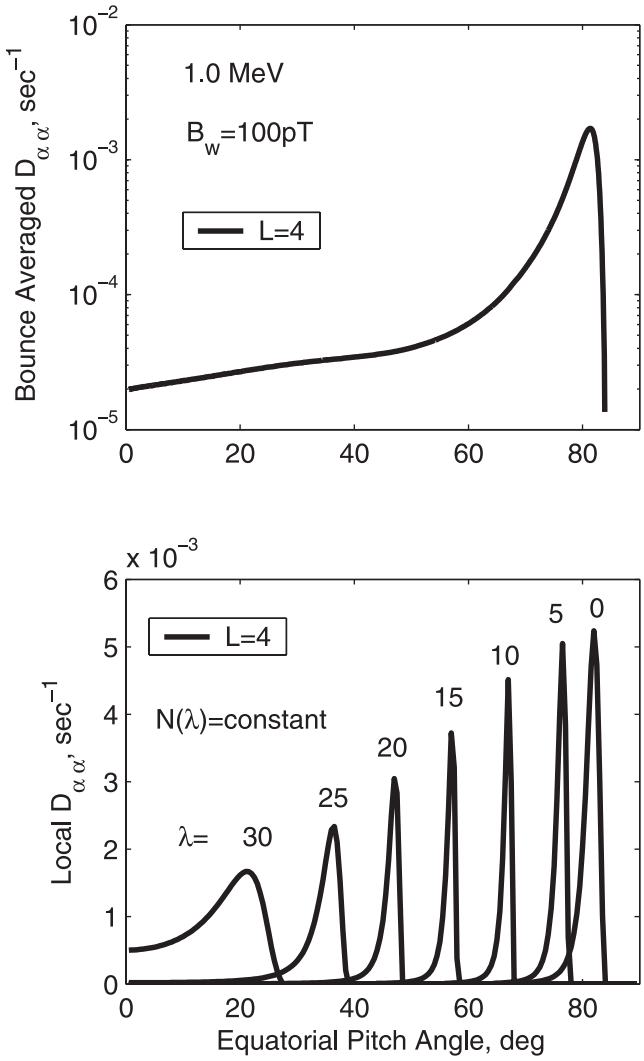

Figure 3. Variation of the local rate of pitch angle scattering with latitude along the bounce orbit of 1 MeV electrons at $L = 4$ (bottom). Bounce-averaged diffusion rates are presented at the top.

approximate results, with exact solutions from the BAS diffusion code PADIE [*Horne et al.*, 2005]. The computations are performed for 1 MeV electrons at $L = 4$, assuming a constant density along the field line. Two exact solutions are shown. The first (dash-dot) has a wave normal distribution confined within 1° of the ambient magnetic field, and only scattering from the dominant ($n = 1$) first-order cylotron harmonic is included. In the second (dashed), the waves are distributed over 30° and all resonances up to the fifth harmonic are included. In our approximate results (solid line) the neglect of ω in the resonance condition (8) and also the approximation on the whistler dispersion relation (11) lead to a misplacement of the local resonant scattering peaks, particularly for equatorial pitch angles near 90°. However, our bounce-averaged scattering rates near the edge of the loss cone are remarkably similar to both exact solutions, indicating that we can estimate electron lifetimes to within a factor of two. Because of the computational efficiency, we will use the approximate solutions to test the sensitivity of lifetimes to key parameters.

[15] First, consider the contribution to MeV microburst loss from local scattering at different latitudes. The lower part of Figure 3 shows local scattering rates at $L = 4$ for a constant density model. Wave frequencies are fixed to the equatorial values listed above, and the waves are also assumed to have amplitudes independent of latitude. Near the equator, resonance with MeV electrons is confined to a very narrow range of pitch angles near 80°. At higher latitude the peak scattering rate diminishes and moves to lower equatorial pitch angles. Significant scattering near the loss cone ($\alpha_{eq} \sim 5°$) only begins to occur at latitudes above 30°. High-latitude chorus is therefore required to produce MeV microbursts. When bounce-averaging is performed, the net rate of scattering is greatly reduced near the loss cone but still gives an effective lifetime comparable to 2 days.

[16] The dependence of scattering lifetimes on L shell and on the adopted latitudinal distribution of density have also been investigated. The top part of Figure 4 indicates a very modest decrease in lifetime over the L range from 3 to 7 for the case of $N(\lambda)$ constant, assuming that wave amplitude remains at 100 pT for all L. For the density model with

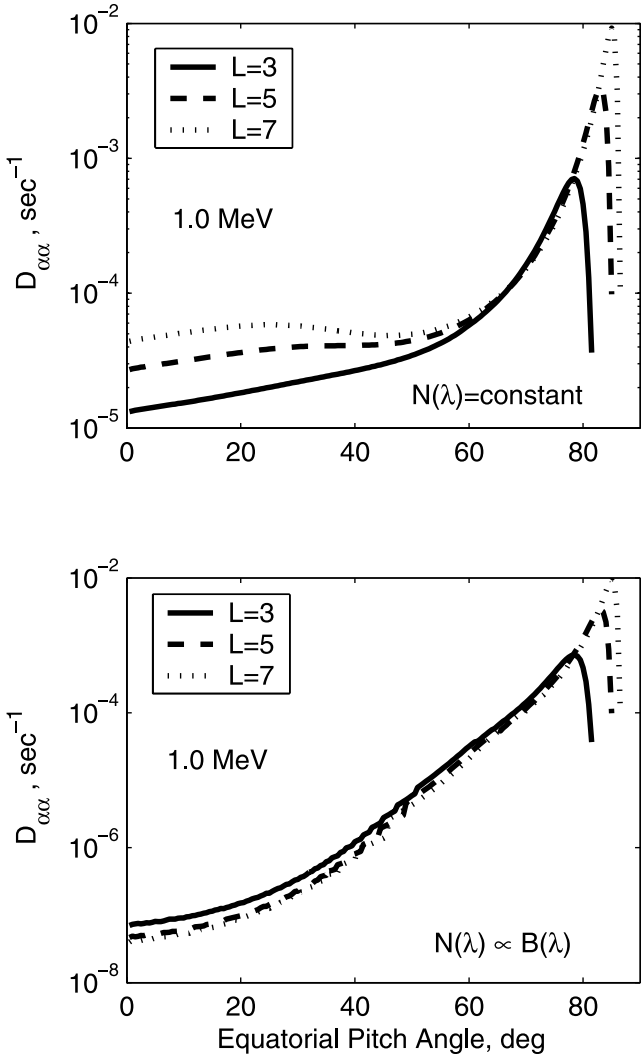

Figure 4. Variation of the bounce-averaged rate of pitch angle scattering with L for a density model with $N(\lambda)$ constant (top) and $N(\lambda) \sim B_0(\lambda)$ (bottom).

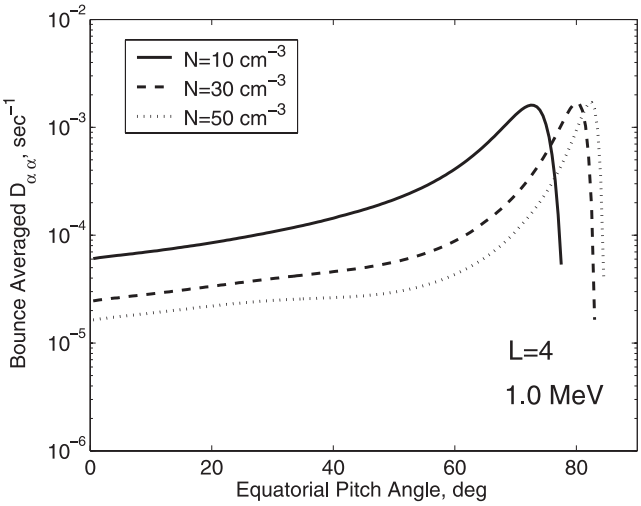

Figure 5. Sensitivity of the bounce-averaged rate of scattering to variations in plasma density. Shorter lifetimes occur during the main phase of a storm when the density is lowest.

$N(\lambda) \sim B_0(\lambda)$, lifetimes become longer than a year, which is clearly unrealistic. The reason for this great difference in scattering rates near the loss cone is the sensitivity of the resonance condition to the parameter $\alpha^* = (\Omega_e/\omega_{pe})^2$, which scales as $B_0^2(\lambda)$ for a constant density model and as $B_0(\lambda)$ when $N(\lambda) \sim B_0(\lambda)$. The more rapid increase in α^* for the constant density model allows MeV electrons to resonate effectively with chorus at smaller latitude, leading to larger bounce-averaged diffusion rates near the loss cone.

[17] During different phases of a storm, plasma density at a given L shell outside the plasmapause can be expected to exhibit substantial variability with MLT [*Sheeley et al.*, 2001]. Lowest densities are expected on the nightside and during the onset of the main phase, as the plasmapause reforms at lower L, and enhanced convection transports plasma of ionospheric origin to the dayside magnetopause. In the storm recovery, ionospheric outflow causes an increase in plasma density, particularly on the dayside. We consequently evaluate the effect of the large variability in trough plasma densities reported by *Sheeley et al.* [2001] on MeV scattering rates. The results shown in Figure 5 indicate that scattering lifetimes are extremely sensitive to changes in density. Lifetimes at $L = 4$ could drop below a day for the lower densities (10/cc) expected during the main phase of a storm and subsequently increase to over 3 days as densities build up to 50/cc during the storm recovery, without any change in the properties of the scattering waves. This conclusion is consistent with the results of *O'Brien et al.* [2004], who showed that microburst loss is far more effective during the storm main phase.

[18] A statistical survey of CRRES chorus emissions [*Meredith et al.*, 2003] indicates that nightside emissions are generally confined to within 15° of the equator, whereas dayside chorus becomes more intense at higher latitudes. We explore the effect of this difference on the precipitation loss of MeV electrons in Figure 6. For this simulation, the amplitude of chorus is held constant at 100 pT, up to a maximum latitude λ_m, and then set to zero at higher latitudes. For the case of waves confined within 15° of the equator, there is no scattering near the loss cone (~5°). We therefore conclude that nightside chorus should not produce MeV microbursts, although scattering can occur at much lower energies. Waves must extend to at least 30° latitude for significant MeV microburst loss. Such intense high-latitude chorus emissions are found on the dayside, particularly in the prenoon sector [*Horne et al.*, 2005] where microbusts are mainly observed [*O'Brien et al.*, 2004].

5. Discussion

[19] Intense chorus emissions which are excited during enhanced convection events are able to resonate with relativistic electrons at high latitudes leading to MeV microburst precipitation. Analysis of microbursts observed on SAMPEX during the main phase of the October 1998 magnetic storm indicates an effective lifetime of about a day throughout the entire outer radiation zone exterior to the plasmapause. Our theoretical study of bounce-averaged diffusion rates yields similar lifetimes for average wave amplitudes comparable to 100 pT, provided that such waves are present at latitudes above 30°. This confines the spatial region of MeV microbursts to the dawn to noon sector, where high-latitude chorus is usually observed [*Meredith et al.*, 2003]. Our theoretical analysis also indicates that the rate of microburst loss is enhanced when magnetospheric plasma densities are lowest, as expected during the main phase of a storm. Microburst loss rates are expected to decrease during the storm recovery, but the persistence of chorus emissions could lead to local acceleration on timescales comparable to a few days [*Horne et al.*, 2005]. Currently, there is little published information on the angular distribution of high-latitude dayside chorus. It is possible that the angular distribution of chorus could change with both latitude (as predicted by ray tracing [e.g., *Horne and Thorne*, 2003]) and MLT. The effect of any change in the wave angular distribution will need to be investigated when better information becomes available.

[20] Interestingly, our determination of the effective lifetime of relativistic electrons by microburst precipitation during the main phase of a storm (~day) is comparable to

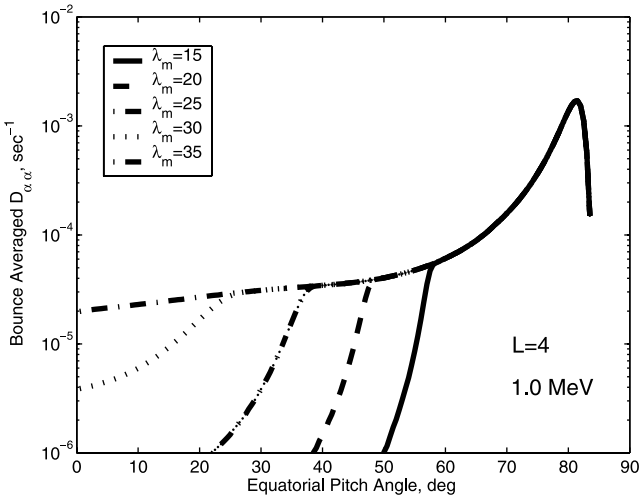

Figure 6. Sensitivity of the bounce-averaged scattering rates near the loss cone to the latitudinal distribution of waves. MeV precipitation requires intense waves above 30° latitude, which are only present in the dusk-noon sector.

the recent calculations for the combined scattering by stormtime plasmaspheric hiss and EMIC waves [*Albert*, 2003; *Summers and Thorne*, 2003], suggesting that all three waves play an important role in stormtime electron dynamics. Outer zone MeV electron lifetimes of less than a day (for storm main phase conditions) have also been reported from radial diffusion modeling [*Shprits and Thorne*, 2004]. Such rapid net rate of loss will compete with any potential acceleration process and needs to be carefully taken into account. It appears that the more rapid loss during the main phase of a storm generally exceeds any acceleration source and thus leads to a net depletion of the relativistic outer zone population. A net increase in MeV electron flux can occur during the recovery of certain storms [*Reeves et al.*, 2003], presumably when source processes dominate over weakened loss mechanisms.

[21] Enhanced radial diffusion [e.g., *Elkington et al.*, 2003] and local stochastic acceleration during resonant interactions with chorus [e.g., *Horne et al.*, 2005] are leading candidates to explain the observed relativistic electron flux enhancements during the storm recovery phase. Both processes are expected to be important due to the observed stormtime enhancement in the power spectral density of ULF and VLF waves [*O'Brien et al.*, 2003]. It is intriguing that scattering by chorus can act simultaneously as a loss mechanism (owing to pitch angle scattering near the loss cone) and as a source of local acceleration. This is possible because the rate of energy diffusion maximizes for pitch angles well away from the loss cone [e.g., *Horne et al.*, 2005], while the bounce-averaged pitch angle diffusion rates minimize near the loss cone (Figure 2). Theoretical modeling [*Thorne et al.*, 2005] has shown that the combined effect of pitch angle and energy diffusion leads to the observed development of flat-topped pitch angle distributions (with steep gradients near the loss cone) [*Horne et al.*, 2003b] and peaks in phase space density [*Green and Kivelson*, 2004]. The effect of radial diffusion needs to be included in future studies by an in-depth analysis with three-dimensional diffusion codes in order to quantify the relative role of each class of wave on stormtime electron dynamics.

[22] **Acknowledgments.** This research was funded in part by NASA grants NAG5-11922 and NNG04GN44G. The work was also supported by NSF GEM grant ATM-0402615. We thank R. Selesnick and M. Looper for assistance with the Polar and SAMPEX data. D. S. acknowledges support from the Natural Sciences and Engineering Research Council of Canada under grant A-0621.

[23] Arthur Richmond thanks Jay Albert and Reiner Friedel for their assistance in evaluating this paper.

References

Albert, J. M. (2003), Evaluation of quasi-linear diffusion coefficients for EMIC waves in a multi-species plasma, *J. Geophys. Res.*, *108*(A6), 1249, doi:10.1029/2002JA009792.

Albert, J. M. (2005), Evaluation of quasi-linear diffusion coefficients for whistler mode waves in a plasma with arbitrary density ratio, *J. Geophys. Res.*, *110*, A03218, doi:10.1029/2004JA010844.

Blake, J. B., M. D. Looper, D. N. Baker, R. Nakamura, B. Kleckert, and D. Hovestadt (1996), New high temporal and spatial measurements by SAMPEX of the precipitation of relativistic electrons, *Adv. Space Res.*, *18*(8), 171.

Elkington, S. R., M. K. Hudson, and A. A. Chan (2003), Resonant acceleration and diffusion of outer zone electrons in an asymmetric geomagnetic field, *J. Geophys. Res.*, *108*(A3), 1116, doi:10.1029/2001JA009202.

Glauert, S. A., and R. B. Horne (2005), Calculation of pitch angle and energy diffusion coefficients with the PADIE code, *J. Geophys. Res.*, *110*, A04206, doi:10.1029/2004JA010851.

Green, J. C., and M. G. Kivelson (2004), Relativistic electrons in the outer radiation belt: Differentiating between acceleration mechanisms, *J. Geophys. Res.*, *109*, A03213, doi:10.1029/2003JA010153.

Horne, R. B., and R. M. Thorne (2003), Relativistic electron acceleration and precipitation during resonant interactions with whistler-mode chorus, *Geophys. Res. Lett.*, *30*(10), 1527, doi:10.1029/2003GL016973.

Horne, R. B., S. A. Glauert, and R. M. Thorne (2003a), Resonant diffusion of radiation belt electrons by whistler-mode chorus, *Geophys. Res. Lett.*, *30*(9), 1493, doi:10.1029/2003GL016963.

Horne, R. B., N. P. Meredith, R. M. Thorne, D. Heyndrickx, R. H. A. Iles, and R. R. Anderson (2003b), Evolution of energetic electron pitch angle distributions during storm time electron acceleration to megaelectronvolt energies, *J. Geophys. Res.*, *108*(A1), 1016, doi:10.1029/2001JA009165.

Horne, R. B., R. M. Thorne, S. A. Glauert, J. M. Albert, N. P. Meredith, and R. R. Anderson (2005), Timescale for radiation belt electron acceleration by whistler mode chorus waves, *J. Geophys. Res.*, *110*, A03225, doi:10.1029/2004JA010811.

Lorentzen, K. R., J. B. Blake, U. S. Inan, and J. Bortnik (2001), Observations of relativistic electron microbursts in association with VLF chorus, *J. Geophys. Res.*, *106*, 6017.

Lyons, L. R., and D. J. Williams (1984), *Quantitative Aspects of Magnetospheric Physics*, Elsevier, New York.

Lyons, L. R., R. M. Thorne, and C. F. Kennel (1971), Electron pitch angle diffusion driven by oblique whistler-mode turbulence, *J. Plasma Phys.*, *6*, 589.

Lyons, L. R., R. M. Thorne, and C. F. Kennel (1972), Pitch angle diffusion of radiation belt electrons within the plasmasphere, *J. Geophys. Res.*, *77*, 3455.

Meredith, N. P., R. B. Horne, R. M. Thorne, and R. R. Anderson (2003), Favored regions for chorus-driven electron acceleration to relativistic energies in the Earths outer radiation belt, *Geophys. Res. Lett.*, *30*(16), 1871, doi:10.1029/2003GL017698.

O'Brien, T. P., K. R. Lorentzen, I. R. Mann, N. P. Meredith, J. B. Blake, J. F. Fennell, M. D. Looper, D. K. Milling, and R. R. Anderson (2003), Energization of relativistic electrons in the presence of ULF power and MeV microbursts: Evidence for dual ULF and VLF acceleration, *J. Geophys. Res.*, *108*(A8), 1329, doi:10.1029/2002JA009784.

O'Brien, T. P., M. D. Looper, and J. B. Blake (2004), Quantification of relativistic electron microbursts losses during the GEM storms, *Geophys. Res. Lett.*, *31*, L04802, doi:10.1029/2003GL018621.

Reeves, G. D., K. L. McAdams, R. H. W. Friedel, and T. P. O'Brien (2003), Acceleration and loss of relativistic electrons during geomagnetic storms, *Geophys. Res. Lett.*, *30*(10), 1529, doi:10.1029/2002GL016513.

Santolik, O., D. A. Gurnett, and J. S. Pickett (2003), Spatio-temporal structure of storm-time chorus, *J. Geophys. Res.*, *108*(A7), 1278, doi:10.1029/2002JA009791.

Sheeley, B. W., M. B. Moldwin, H. K. Rassoul, and R. R. Anderson (2001), An empirical plasmasphere and trough density model: CRRES observations, *J. Geophys. Res.*, *106*, 25,631.

Shprits, Y. Y., and R. M. Thorne (2004), Time-dependent radial diffusion modeling of relativistic electrons with realistic loss rates, *Geophys. Res. Lett.*, *31*, L08805, doi:10.1029/2004GL019591.

Summers, D., and R. M. Thorne (2003), Relativistic electron pitch angle scattering by electromagnetic ion cyclotron waves during geomagnetic storms, *J. Geophys. Res.*, *108*(A4), 1143, doi:10.1029/2002JA009489.

Thorne, R. M., R. B. Horne, S. A. Glauert, N. P. Meredith, Y. Y. Shprits, D. Summers, and R. R. Anderson (2005), The influence of wave-particle interactions on relativistic electron dynamics during storms, in *Inner Magnetosphere Interactions: New Perspectives From Imaging*, *Geophys. Monogr. Ser.*, vol. 159, edited by J. Burch, M. Schulz, and H. Spence, AGU, Washington, D. C.

Tsurutani, B. T., and E. J. Smith (1977), Two types of magnetospheric ELF chorus and their substorm dependences, *J. Geophys. Res.*, *82*, 5112.

Vampola, A. L. (1996), Outer zone energetic electron environment update, *Final Rep. 151351*, Eur. Space Agency, Noordwijk, Netherlands.

R. B. Horne, British Antarctic Survey, Natural Environment Research Council, Madingley Road, Cambridge, CB3 0ET, UK. (r.horne@bas.ac.uk)

T. P. O'Brien, Space Science Department, The Aerospace Corporation, El Segundo, CA 90009-2957, USA. (paul.obrien@aero.org)

Y. Y. Shprits and R. M. Thorne, Department of Atmospheric and Oceanic Sciences, University of California, Los Angeles, 405 Hilgard Avenue, Los Angeles, CA 90095-1565, USA. (yshprits@atmos.ucla.edu; rmt@atmos.ucla.edu)

D. Summers, Department of Mathematics and Statistics, Memorial University of Newfoundland, St. John's, Newfoundland, Canada, A1C 5S7. (dsummers@math.mun.ca)